

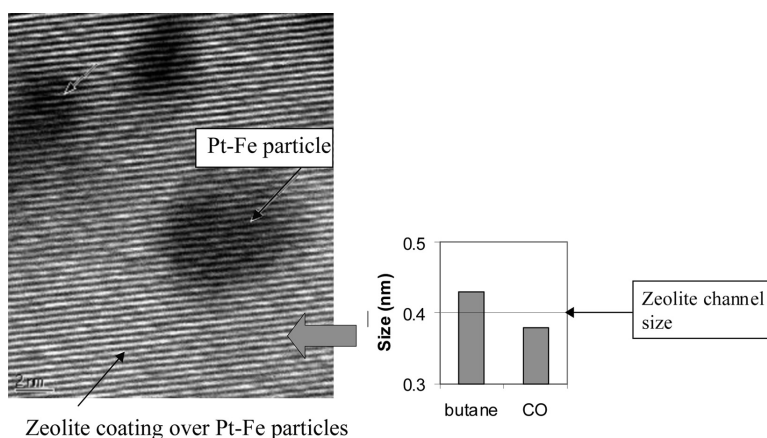
Communication

**Active-Site Coating for Molecular Discrimination in Heterogeneous Catalysis**

Paul Collier, Stan Golunski, Chan Malde, John Breen, and Robbie Burch

*J. Am. Chem. Soc.*, **2003**, 125 (41), 12414-12415 • DOI: 10.1021/ja037136s • Publication Date (Web): 20 September 2003

Downloaded from <http://pubs.acs.org> on March 29, 2009



**More About This Article**

Additional resources and features associated with this article are available within the HTML version:

- Supporting Information
- Links to the 4 articles that cite this article, as of the time of this article download
- Access to high resolution figures
- Links to articles and content related to this article
- Copyright permission to reproduce figures and/or text from this article

[View the Full Text HTML](#)

## Active-Site Coating for Molecular Discrimination in Heterogeneous Catalysis

Paul Collier,<sup>\*,†</sup> Stan Golunski,<sup>†</sup> Chan Malde,<sup>†</sup> John Breen,<sup>‡</sup> and Robbie Burch<sup>‡</sup>

Johnson Matthey Technology Centre, Blount's Court, Sonning Common, Reading RG4 9NH, U.K., and School of Chemistry, Queen's University Belfast, David Keir Building, Belfast BT9 5AG, U.K.

Received July 8, 2003; E-mail: collipj@matthey.com

Heterogeneous catalysts often lack the ability to convert only specific molecules in a mixture of reactants. Although this lack of chemo-discrimination can be partially overcome by chemically modifying the catalyst surface,<sup>1</sup> tuning the operating conditions,<sup>2</sup> or designing enzyme mimics,<sup>3</sup> substantial improvements are often not possible. In principle, a much simpler approach is to control the diffusion of reactants to the active sites, by enveloping the catalyst in a selectively permeable membrane.<sup>4</sup> Uniform thin coverings of membrane materials have proved exceptionally difficult to achieve in the past, and so multiple layers of crystallites have been used instead to form coherent coatings.<sup>5–7</sup> As compared to the prior art, we have used a simpler and more scaleable preparative method to apply a zeolite (4A) to a supported catalyst. Our method requires a blanket charge-reversal step, with no pore masking (as used by Hedlund et al.),<sup>7</sup> before the catalyst is brought into contact with the zeolite gel. Although multiple layers of crystallites are visible by SEM, the coated catalyst retains its ability to discriminate perfectly between CO and butane even after it has been deliberately crushed. High-resolution TEM reveals that, below the crystallite layers, the active sites of the catalyst are coated in an ultrathin but coherent zeolite membrane.

In the modern route to maleic anhydride, *n*-butane is widely used as the organic feedstock, which is catalytically converted to the product by partial oxidation.<sup>8–10</sup> If the process is operated at high selectivity to maleic anhydride, the per-pass conversion of butane is low (10–15%), which requires the product stream to be cooled below 200 °C (to condense the maleic anhydride) before it is fed back into the reactor.<sup>10–13</sup> In addition to unreacted butane, the recycled gas stream also contains some CO and CO<sub>2</sub>, that is, the nonselective products of butane oxidation. The CO<sub>2</sub> behaves as an inert species in this process, but the CO deactivates the partial-oxidation catalyst, and so needs to be removed during the recycle step.<sup>14</sup> The challenge lies in developing an additional catalyst that will clean up CO by oxidizing it at ≤200 °C, without wasting any of the butane. The sodium form of zeolite A (effective channel size: 0.4 nm) offers the prospect of controlling access to a clean-up catalyst by allowing permeation of CO (kinetic diameter: 0.38 nm) while excluding *n*-butane (kinetic diameter: 0.43 nm).

As we and others have found,<sup>5</sup> the formation of a continuous coating of zeolite is not easy to achieve over a silica- or alumina-supported catalyst using conventional hydrothermal crystallization techniques. The surface charge of silica, alumina, and many common zeolites is negative at basic pH (typical zeolite synthesis conditions),<sup>13,14</sup> which means that there is an electrostatic barrier preventing the growth of zeolite overlayers on silica- or alumina-based catalysts. To overcome this, we have simply reversed the surface charge of the entire exposed surface of our chosen clean-up catalyst (5% Pt–0.5% Fe, by weight, supported on small highly macroporous silica spheres), using a copolymer of acrylamide and

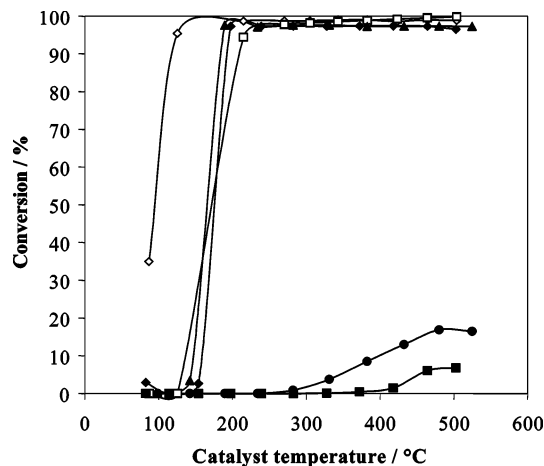


**Figure 1.** Species-selective oxidation of CO in the presence of butane: uncoated Pt–Fe/SiO<sub>2</sub> (—◇— CO conversion, —□— butane conversion); zeolite A coated Pt–Fe/SiO<sub>2</sub> (—◆— CO conversion, —■— butane conversion); crushed sample of zeolite A coated Pt–Fe/SiO<sub>2</sub> (—▲— CO conversion, —●— butane conversion).

the methyl chloride quaternary salt of 2-(dimethylamino)ethyl acrylate.<sup>15</sup> The polymer species are strongly adsorbed on the support, by the electrostatic attraction between the quaternary ammonium groups of the adsorbate and the oxide ions at the support surface, resulting most probably in a flat conformation.<sup>16</sup> The presence of excess quaternary ammonium groups imparts an overall positive charge to the polymer-covered support surface, including, we believe, the inside of the pores where most of the catalytically active sites are located. The zeolite is then crystallized on the modified surface, followed by a thermal treatment, which removes the polymer and fixes the zeolite as a rigid overlayer.

The catalytic activity of the Pt–Fe/SiO<sub>2</sub>–zeolite A composite material was compared to that of the uncoated catalyst, for CO oxidation in the presence of excess butane (Figure 1). The degree of chemo-discrimination shown by the uncoated catalyst was low. Although the oxidation of butane started at a temperature 50 °C higher than that of CO, it would be very difficult to use this catalyst to oxidize the CO without removing any of the butane, even in a well-controlled isothermal reactor.

Significantly, the presence of the zeolite A membrane eliminated any butane combustion below about 400 °C, but still allowed the CO to be oxidized below 200 °C. Even above 400 °C, the butane-conversion profile was not typical of combustion, but was more characteristic of hydrocarbon cracking taking place on the zeolite surface. In this composite material, the zeolite membrane acts to exclude completely the relatively large butane molecules, while only slightly inhibiting the transport of CO to the catalytically active sites.

Our initial hypothesis was that the observed diffusional control was being provided by a relatively thick coating of cuboid zeolite crystallites, which SEM showed enveloping the exterior surface of

<sup>†</sup> Johnson Matthey Technology Centre.

<sup>‡</sup> Queen's University Belfast.

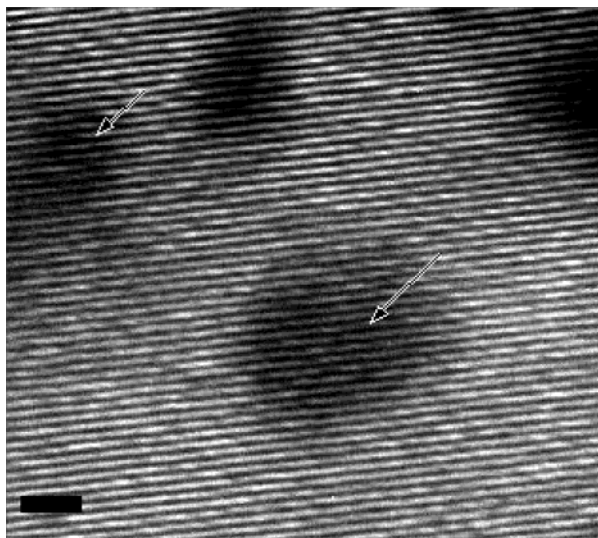


**Figure 2.** TEM image of zeolite A membrane covering Pt–Fe particles (size bar 2 nm).

each macroscopic catalyst sphere. Although the coating was robust enough to withstand repeated thermal cycling, we expected that the diffusional control would be substantially reduced by deliberately fracturing the coating. However, even after grinding the 3.2 mm spheres to a powder in the 250–800  $\mu\text{m}$  particle size range, the catalytic performance (Figure 1) did not revert to that of the uncoated catalyst. The CO-oxidation profile was almost identical in position and shape to that of the uncrushed material, with no sign of a lowering in the onset temperature that would indicate a measurable number (i.e., 1%) of uncovered metal sites. The conversion of butane started at a lower temperature, but was still consistent in shape with hydrocarbon-cracking (now on a larger exposed area of zeolite) and not with combustion on the metal sites.

SEM analysis of deliberately broken spheres showed that zeolite crystallites were present within the macropore structure of the spheres. This was confirmed by EDAX (energy dispersive analysis of X-rays) mapping, which showed deep penetration of aluminum-containing species into the pores of the spheres. Collectively, the results suggested that the zeolite crystallites form a coating over all of the available external and internal surfaces of the spheres to a depth of typically 10–20  $\mu\text{m}$ . HRTEM revealed that, in addition to the cuboid crystallites observed by SEM, zeolite A is also present in the composite material as 70 nm wide needlelike crystals. These needles appear to be present throughout the sample and are of variable length, typically between 100 and 700 nm.

However, the most significant discovery made by HRTEM was that the individual Pt–Fe particles (typically 4–10 nm in diameter) are covered by an extended 50–70 nm thick membrane. The interplanar spacing within the membrane is 0.354 nm, corresponding to the 2,2,2 Bragg plane of zeolite A. The membrane is substantially monocrystalline and can only be imaged by careful focusing above the plane of the metal particles (Figure 2).

Our catalytic tests have demonstrated that using total surface charge-reversal (i.e., without pore-screening) to apply zeolite A to a Pt–Fe/SiO<sub>2</sub> catalyst leads to impressive chemo-discrimination between CO and excess butane. In the early part of this work, our conceptual model of this composite material was based on the assumption that the 2–3  $\mu\text{m}$  cuboid crystallites, observed by SEM, form a relatively thick coating over all of the external surfaces and, hence, over the pore structure containing the catalytically active sites. We have since revised this model in light of the HRTEM evidence and propose that the cause of the molecular discrimination lies much closer to the local environment of the active sites. Even when the exterior macroscale coating is damaged, the active sites (located on the dispersed metal particles) are protected by a thin coherent layer of zeolite, which controls the entry and exit of gas-phase species. Our preparative method has allowed the zeolite to track the dispersed metal particles into the pore structure of the support material. We believe that this is the first time this effect has been demonstrated.

**Acknowledgment.** We thank Neil Edwards, Alan Stubbs, and Steve Spratt, of the Johnson Matthey Technology Centre, for  $\zeta$ -potential measurements and electron microscopy, and Marc Coleman, of Queen's University Belfast, for assistance in the catalytic activity measurements.

**Supporting Information Available:** Rationale, catalyst preparation, electron microscopy, and catalyst testing (PDF). This material is available free of charge via the Internet at <http://pubs.acs.org>.

## References

- (1) Grisel, R. J. H.; Westrate, C. J.; Goossens, A.; Craje, M. W. J.; van der Kraan, A. M.; Nieuwenhuys, B. E. *Catal. Today* **2002**, *72*, 123–132.
- (2) Sedmak, G.; Hocevar, S.; Levec, J. *J. Catal.* **2003**, *213*, 135–150.
- (3) De Vos, D. E.; Sels, B. F.; Jacobs, P. A. *CATTECH* **2002**, *6*, 14–29.
- (4) van der Puil, N.; Creighton, E. J.; Rodenburg, E. C.; Sie, T. S.; van Bekkum, H.; Jansen, J. C. *J. Chem. Soc., Faraday Trans.* **1996**, *92*, 4609–4615.
- (5) van der Puil, N.; Dautzenberg, F. M.; van Bekkum, H.; Jansen, J. C. *Microporous Mesoporous Mater.* **1999**, *27*, 95–106.
- (6) Jansen, J. C.; Koegler, J. H.; van Bekkum, H.; Calis, H. P. A.; van den Bleek, C. M.; Kapteijn, F.; Moulijn, J. A.; Geus, E. R.; van der Puil, N. *Microporous Mesoporous Mater.* **1998**, *21*, 213–226.
- (7) Hedlund, J.; Sterte, J.; Anthonis, M.; Bons, A.-J.; Carstensen, B.; Corcoran, N.; Cox, D.; Deckman, H.; De Gijst, W.; de Moor, P.-P.; Lai, F.; McHenry, J.; Mortier, W.; Reinoso, J.; Peters, J. *Microporous Mesoporous Mater.* **2002**, *52*, 179–189.
- (8) Volta, J. C. *C. R. Acad. Sci., Ser. II Fascicule C—Chimie* **2000**, *3*, 717–723.
- (9) Madeira, L. M.; Portela, M. F. *Catal. Rev.-Sci. Eng.* **2002**, *44*, 247–286.
- (10) Felthouse, T. R.; Burnett, J. C.; Horrell, B.; Mummey, M. J.; Kuo Y.-J., <http://www.huntsman.com/petrochemicals/Media/KOMaleic.pdf>, 2001.
- (11) Hassan, T., US 5011945, 1991.
- (12) O'Sullivan, D. *Chem. Eng. News* **1992**, *70*, 6–6.
- (13) Stadig, W. *Chem. Process.* **1992**, *55*, 26–31.
- (14) Gai P. L.; Boyes E. D. In *Electron Microscopy in Heterogeneous Catalysis*; Cantor, B., Goringe, M. J., Eades, J. A., Eds.; Institute of Physics: Bristol, 2003; pp 110–124.
- (15) Goodman, K. E.; Hayes, J. W.; Malde, C. N.; Petch, M. I., EP 0 878 233, 1998.
- (16) Fan, A.; Turro, N. J.; Somasundaran, P. *Colloids Surf., A* **2000**, *162*, 141–148.

JA037136S